

Characterization and inference of weighted graph topologies from observations of diffused signals

Bastien Padeloup, Vincent Gripon, Grégoire Mercier, Dominique Pastor, and Michael G. Rabbat

Abstract—In the field of signal processing on graphs, a key tool to process signals is the graph Fourier transform. Transforming signals into the spectral domain is accomplished using the basis of eigenvectors of the graph Laplacian matrix. Such a matrix is dependent on the topology of the graph on which the signals are defined. Therefore it is of paramount importance to have a graph available. We consider the problem of inferring the graph topology from observations of signals. In this article we model the observations as being measured after a few steps of diffusing signals that are initially mutually independent and have independent entries. We propose a way to characterize and recover the possible graphs used for this diffusion. We show that the space of feasible matrices on which mutually independent signals can have evolved, based on the observations, is a convex polytope, and we propose two strategies to choose a point in this space as the topology estimate. These strategies enforce the selection of graphs that are, respectively, simple or sparse. Both methods can be formulated as linear programs and hence solved efficiently. Experiments suggest that in the ideal case when we are able to retrieve the exact covariance matrix of the signal, we are able to recover the graph on which the signals were diffused, with no error. We also apply our method to a synthetic case in which a limited number of signals are obtained by diffusion on a known graph, and show that we are able to recover a graph that is very close to the ground truth one, with an error decreasing as the number of observations increases. Finally, we illustrate our method on audio signals, and show that we are able to recover a graph that is globally one-dimensional.

I. INTRODUCTION

In many applications, such as brain imaging [1] and hyperspectral imaging [2], it is convenient to model and/or classify the relationships among the components of the signals studied using a graph. Classical methods to obtain such a graph are generally based on thresholding the empirical covariance matrix of the studied signals [3], or by recovering a sparse precision matrix for these signals using tools such as the graphical lasso [4]. In recent years, the field of signal processing on graphs has emerged with the aim of generalizing the Fourier approach to non-linear domains. One of its possible applications is to explain the link between the studied signals and what would be a graph describing the support on which they evolve.

This was supported by the European Research Council under the European Union's Seventh Framework Programme (FP7/2007-2013) / ERC grant agreement n° 290901, and by the Natural Sciences and Engineering Research Council of Canada through grant RGPAS 429296-12.

B. Padeloup, V. Gripon, G. Mercier, and D. Pastor are with UMR CNRS Lab-STICC, Télécom Bretagne, 655 Avenue du Technopole, 29280, Plouzané, France. Email: {name.surname}@telecom-bretagne.eu.

M.G. Rabbat is with the Department of Electrical and Computer Engineering, McGill University, 3480 University Street, Montréal, H3A 0E9, Canada. Email: michael.rabbat@mcgill.ca.

A possible approach to obtain such a graph is to represent the support on which mutually independent signals with independent entries would have evolved to cause the observation of the studied signals. However, in practical cases, finding the perfect graph modeling this support is very complicated, since most propagation processes imply non-linearities. An example is the propagation of a disease in a population: components of the signals are binary, modeling whether the persons are infected or not. Therefore, one propagation step cannot simply be modeled by a connectivity matrix. A common and efficient approach to deal with this complexity is to approximate this complicated propagation process with a simplified linear diffusion model.

Assuming that the signals to study are issued from the linear diffusion of initially mutually independent signals with independent entries, we address the following questions:

- How can we characterize an adapted diffusion matrix from a set of observed signals?
- Given a set of potential diffusion matrices, how do we select one to explain the given signals?

To answer these questions, we first introduce some desired properties of the diffusion support. Enforcing these properties can be done by respecting a set of linear inequality constraints. A consequence of this is that the set of admissible diffusion matrices is a convex polytope.

Then, we study two strategies to select a point in this polytope. The first one aims to recover a simple graph, *i.e.*, a graph for which there are no loops on the vertices. This can be done by minimizing the trace of the objective matrix, and reduces to solving a linear programming problem. The second method we study is based on recovering a sparse matrix. We show that this strategy too can be addressed using a linear programming problem by minimizing the ℓ_1 norm of the target matrix.

This paper is organized as follows. First, we introduce in Section II the problem we address in this article, and present the required notions and vocabulary that are necessary for a full understanding of our work. Then, in Section III, we review the work that has been done in graph recovering from the observation of signals. In Section IV, we study the desired properties that characterize the admissible diffusion matrices. Then, in Section V, we analyze two possible methods to select an admissible diffusion matrix explaining the observed signals, based on some chosen criteria. Finally, in Section VI, we illustrate the reconstruction process on synthetic data and validate our method on audio signals.

II. PROBLEM FORMULATION

In this article, we consider a set of N random variables (vertices) of interest. Our objective is, given a set of M realizations (signals) of these variables, to infer a graph structure representing the underlying topology on which mutually independent signals with independent entries could have evolved to cause the given M observations.

Definition 1 (Graph): A graph \mathcal{G} is a pair $(\mathcal{V}, \mathcal{E})$ in which $\mathcal{V} = \{1, \dots, N\}$ is a set of N vertices and $\mathcal{E} \subseteq \mathcal{V} \times \mathcal{V}$ is a set of edges. In the remainder of this document, we consider positively weighted undirected graphs. Therefore, we make no distinction between edges (u, v) and (v, u) . By abusing notations, we denote such an edge $\{u, v\}$. A convenient way to represent \mathcal{G} is through its adjacency matrix

$$\mathbf{W}(u, v) \triangleq \begin{cases} \alpha_{uv} & \text{if } \{u, v\} \in \mathcal{E} \\ 0 & \text{otherwise} \end{cases}; \alpha_{uv} \in \mathbb{R}_+; \forall u, v \in \mathcal{V}.$$

A signal on such a graph can be seen as a value attached to every vertex in \mathcal{V} .

Definition 2 (Signal): A signal \mathbf{x} on a graph \mathcal{G} of N vertices is a vector in \mathbb{R}^N .

A widely-studied matrix that allows the study of the propagation of signals on a graph \mathcal{G} is the normalized Laplacian of \mathcal{G} . The eigenvectors of this particular matrix can be used as a Fourier basis to provide a spectral representation of the signals defined on \mathcal{G} [5], [6].

Definition 3 (Normalized Laplacian): The normalized Laplacian \mathbf{L} of a graph \mathcal{G} with adjacency matrix \mathbf{W} is a differential operator on \mathcal{G} , defined by $\mathbf{L} \triangleq \mathbf{I} - \mathbf{D}^{-\frac{1}{2}} \mathbf{W} \mathbf{D}^{-\frac{1}{2}}$; where \mathbf{D} is the diagonal matrix of degrees of the vertices: $\mathbf{D}(u, u) \triangleq \sum_{v \in \mathcal{V}} \mathbf{W}(u, v)$; $\forall u \in \mathcal{V}$, and \mathbf{I} is the identity matrix of size N .

An interpretation of this matrix is to consider the propagation of a signal \mathbf{x} on \mathcal{G} using \mathbf{L} . By definition, $\mathbf{L}\mathbf{x} = \mathbf{I}\mathbf{x} - (\mathbf{D}^{-\frac{1}{2}} \mathbf{W} \mathbf{D}^{-\frac{1}{2}})\mathbf{x}$. Therefore, the normalized Laplacian models the variation of a signal \mathbf{x} when diffused through one step of a diffusion process represented by $\mathbf{D}^{-\frac{1}{2}} \mathbf{W} \mathbf{D}^{-\frac{1}{2}}$. In the remainder of this article, we call $\mathbf{T} \triangleq \mathbf{D}^{-\frac{1}{2}} \mathbf{W} \mathbf{D}^{-\frac{1}{2}}$ the *diffusion matrix* of \mathcal{G} .

By construction, the diffusion matrix \mathbf{T} of \mathcal{G} is a symmetric, non-negative matrix, with $\mathbf{T}(u, v) = 0 \Leftrightarrow \mathbf{W}(u, v) = 0$; $\forall u, v \in \mathcal{V}$. A consequence of this property is that knowledge of \mathbf{T} implies knowledge of the associated graph if \mathbf{W} is a binary matrix, i.e. if $\forall u, v \in \mathcal{V} : \{u, v\} \in \mathcal{E} \Leftrightarrow \alpha_{uv} = 1$ in Definition 1.

Using the previously introduced definitions, we can formulate the problem we address in this paper as follows. Let $\mathbf{X} = (\mathbf{x}_1, \dots, \mathbf{x}_M)$, $\mathbf{x}_i \in \mathbb{R}^N$, be a matrix of M observations, one per column. Let $\mathbf{Y} = (\mathbf{y}_1, \dots, \mathbf{y}_M)$, $\mathbf{y}_i \in \mathbb{R}^N$, be an unknown matrix of M mutually independent signals with independent entries; i.e., the entries $\mathbf{Y}(i, j)$ are zero-mean, independent random variables. Let $\mathbf{k} \in \mathbb{R}_+^M$ be an unknown vector of M positive numbers. Given \mathbf{X} , we aim to find a diffusion matrix¹ $\hat{\mathbf{T}}$ such that there exist \mathbf{Y} and \mathbf{k} and $\forall i \in \{1, \dots, M\} : \mathbf{x}_i = \hat{\mathbf{T}}^{\mathbf{k}(i)} \mathbf{y}_i$.

¹Throughout this article we will denote recovered/estimated quantities using a hat.

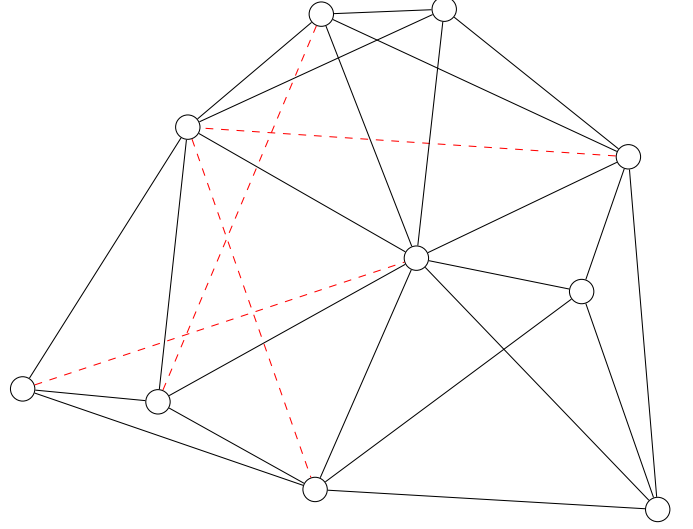


Figure 1. Graph recovered from a thresholding of the covariance matrix. The black edges are those that are present in the ground truth graph, as well as in the recovered one. The red ones are those only present in the recovered graph. θ is chosen as the highest threshold value such that every edge of the groundtruth graph exists in the thresholded covariance matrix.

III. RELATED WORK

In this section we review related approaches in the literature to reconstruct a graph from the observation of signals.

A. Thresholding the covariance matrix

The covariance matrix $\Sigma_{\mathbf{X}}$ of a matrix of zero-mean signals \mathbf{X} , defined as $\Sigma_{\mathbf{X}} \triangleq \mathbb{E}[\mathbf{X}\mathbf{X}^T]$, represents how much the signal components tend to *move together* across all signal instances. Therefore, variables that are very similar will have a large coefficient in the covariance matrix.

Also, two variables that are highly related to a third one will have a non-negligible coefficient in $\Sigma_{\mathbf{X}}$, even though there is no direct link between these two variables. Since the entries in $\Sigma_{\mathbf{X}}$ associated to such variables are generally lower than those associated to existing edges in the graph, a solution to obtain a sparse covariance matrix is to apply a threshold θ to the entries of the empirical covariance matrix to remove the non-significant entries:

$$\Sigma_{\mathbf{X}}/\theta \triangleq \begin{cases} \Sigma_{\mathbf{X}}(i, j) & \text{if } \Sigma_{\mathbf{X}}(i, j) > \theta \\ 0 & \text{otherwise} \end{cases}. \quad (1)$$

When considering signals on a graph, this reduces to considering the covariance matrix as a transitive closure of the graph, and to remove the edges that represent these indirect links among the vertices. To illustrate this, let us consider the example in Fig. 1. Here, we proceed as follows: let \mathbf{W} be the adjacency matrix of a known graph, and let \mathbf{X} be a matrix of signals that are diffused on it, as introduced in Section II. We choose a threshold parameter θ such that every edge of \mathbf{W} exists in $\Sigma_{\mathbf{X}}/\theta$, regardless of the weights. The red edges are those that exist in $\Sigma_{\mathbf{X}}/\theta$, but not in \mathbf{W} .

As we can see, these additional edges link vertices that have a third vertex in common, and are therefore residuals of the transitive closure that could not be removed using a

thresholding, without forcing the removal of some ground truth edges. Therefore, a simple thresholding is generally not sufficient to retrieve a correct graph from the covariance matrix, and one needs to use more elaborate techniques.

B. Graphical lasso based methods

A widely-used approach to recover a graph from data is the *graphical lasso* [4], which recovers a sparse inverse covariance matrix $\hat{\Theta}$ under the assumption that the data are observations from a multivariate Gaussian distribution. The core of this method consists in solving the optimization problem,

$$\hat{\Theta} = \underset{\Theta \geq 0}{\operatorname{argmin}} \left(\operatorname{tr}(\mathbf{S}\Theta) - \log \det(\Theta) + \lambda \sum_{j \neq k} |\Theta_{jk}| \right), \quad (2)$$

where \mathbf{S} is the sample covariance matrix and λ is a regularization parameter. Friedman *et al.* [4] show that this optimization problem can be efficiently solved and it leads to a fast reconstruction of $\hat{\Theta}$.

What makes this method interesting, in addition to its fast convergence toward a sparse solution, is a previous result from Dempster [7]. In the *covariance selection model*, Dempster proposes that the inverse covariance matrix should have numerous null off-diagonal entries. An intuitive interpretation of this is that the indirect links among the variables should be removed to only depict the direct links among the signal components. Such direct relations among variables can then naturally be associated to the edges of the graph to be recovered.

Numerous variations of this technique have been developed [8]–[11], and several applications have been using graphical lasso-based methods for reconstructing a graph from signals. Examples can be found for instance in the fields of neuroimaging [12], [13] or traffic modeling [14].

In our study, we want to provide a way to represent a graph being the diffusion support of signals. Since the graphical lasso provides information on the direct correlations among the observed variables, the recovered graph can be seen as functional, while we focus on a more structural approach. For this reason, the graphical lasso may provide negative correlation values, and does not apply in our case.

C. Smoothness based methods

Another approach was recently proposed by Dong *et al.* [15] which aims to recover a graph enforcing a smoothness property for the signals. A desirable property for a graph on which signals are defined is that vertices linked with an edge should bear similar signal values, thus enforcing *natural* signals on this graph to be low-frequency. A simple measure of smoothness for a signal \mathbf{x} can be described using the quadratic form of the non-normalized graph Laplacian $\mathbf{L} \triangleq \mathbf{D} - \mathbf{W}$ [6]:

$$S(\mathbf{x}) \triangleq \mathbf{x}^\top \mathbf{L} \mathbf{x} = \sum_{\{u,v\} \in \mathcal{E}} \mathbf{W}(u,v) (\mathbf{x}(u) - \mathbf{x}(v))^2. \quad (3)$$

Note that an equation similar to (3) holds when using the normalized Laplacian, after rescaling the entries $\mathbf{x}(u)$ and $\mathbf{x}(v)$ by the square root of the degree of the associated vertex.

From this equation, we can see that the lower $S(\mathbf{x})$ is, the more regular are the components of \mathbf{x} on the graph. In order to find a graph Laplacian — hence the associated adjacency matrix — that minimizes S for a set of signals, the authors introduce an optimization problem, and propose an iterative algorithm to converge to a local solution.

The main interest of this method when compared to graphical lasso-based approaches is the fact that Dong *et al.* succeed in recovering a valid graph Laplacian. For this reason, their method provides a valid graph that can model the support on which signals can evolve, which may fit to our needs.

Dong *et al.* [15] study the case when observed signals should be smooth on the graph, and they propose a method for selecting a particular solution from the space of admissible solutions based on a smoothness-promoting criterion. In the approach we propose in this paper, we propose a more generic approach to characterize the possible space of admissible graphs. Studying the localization of the solution of the approach from Dong *et al.* in this space is an interesting direction for future work.

Enforcing the smoothness property for signals defined on a graph has also been considered by Shivaswamy and Jebara [16], where a method is proposed to jointly learn the kernel of a SVM classifier and optimize the spectrum of the Laplacian to improve this classification.

Contrary to our approach, Shivaswamy and Jebara [16] study a semi-supervised case, in which the spectrum of the Laplacian is learned based on a set of labeled examples.

D. Diffusion based methods

Recently we proposed a third approach to recover a graph from diffused signals. In [17] we study a particular case of the problem we consider here, namely when \mathbf{k} is a known constant vector. Let K denote the value in every entry of this vector.

In [17] we have shown that the covariance matrix of the observations is equal to \mathbf{T}^{2K} . This implies that we need to recover a particular root of the covariance matrix to obtain \mathbf{T} . In more details, if \mathbf{Y} is a matrix of mutually independent signals with independent entries, $\mathbf{X} = \mathbf{T}^K \mathbf{Y}$, and $\Sigma_{\mathbf{X}}$ is the covariance matrix of \mathbf{X} , we have:

$$\begin{aligned} \Sigma_{\mathbf{X}} &= \mathbb{E} [\mathbf{X} \mathbf{X}^\top] \\ &= \mathbb{E} [\mathbf{T}^K \mathbf{Y} \mathbf{Y}^\top \mathbf{T}^{K^\top}] \\ &= \mathbf{T}^K \mathbb{E} [\mathbf{Y} \mathbf{Y}^\top] \mathbf{T}^{K^\top} \\ &= \mathbf{T}^{2K}, \end{aligned} \quad (4)$$

using the independence of \mathbf{Y} and the symmetry of \mathbf{T} .

Thanks to K being known, one could then retrieve a matrix $\hat{\mathbf{T}}$ by diagonalizing $\Sigma_{\mathbf{X}}$, taking the $2K$ -square root of the obtained eigenvalues, and solving a linear optimization problem to recover their missing signs.

We have illustrated this reconstruction process on synthetic cases, where we generate a graph \mathcal{G} and diffuse M mutually independent signals with independent entries on it using the

associated \mathbf{T}^K to obtain \mathbf{X} [17]. Our experiments demonstrate that when M is sufficiently high to have the empirical covariance $\widehat{\Sigma}_{\mathbf{X}}$ equal to $\Sigma_{\mathbf{X}}$ (by using \mathbf{T}^{2K}), we can successfully recover $\widehat{\mathbf{T}} = \mathbf{T}$.

While providing interesting results, this previous work has two principal limitations:

- 1) The number of diffusion steps \mathbf{k} is constant and known, which is a limiting assumption since in practical applications signals may be obtained after a variable, unknown number of diffusion steps. In this work, we remove this assumption. This implies a change of algorithm, since taking the $2K$ -square root of the eigenvalues of $\Sigma_{\mathbf{X}}$ is no longer possible.
- 2) The number of observations M is infinite so we can have $\widehat{\Sigma}_{\mathbf{X}} = \mathbf{T}^{2K}$. We also address this assumption in this paper and show that the higher M is, the closer the recovered graph will be to the ground truth. If M is too small to have $\widehat{\Sigma}_{\mathbf{X}} \approx \Sigma_{\mathbf{X}}$, we show that there still exists a correspondence between the ground truth diffusion matrix and the recovered one.

Finally, we note that there exist methods that aim to recover a graph from the knowledge of the spectrum of its Laplacian [18]. However, here we do not assume that such information is available.

IV. CHARACTERIZATION OF THE SPACE OF ADMISSIBLE DIFFUSION MATRICES

A. Signal processing on graphs

One of the cornerstones of signal processing on graphs is the analogy between the notion of frequency in classical signal processing and the eigenvalues of the Laplacian (either in its normalized form or not). As a matter of fact, the eigenvectors of the Laplacian of a binary ring graph correspond to the classical Fourier modes (see *e.g.*, [6] for a detailed explanation). The lowest eigenvalues are analog to low frequencies, while higher ones correspond to higher frequencies. Using this analogy, researchers have then successfully been able to use graph signal processing techniques on non-ring graphs (*e.g.*, [19], [20]).

To be able to do so, the Laplacian matrix of the studied graph must be diagonalizable. Although it is sufficient, but not necessary, condition for diagonalization, we enforce the symmetry of the normalized Laplacian \mathbf{L} by only considering undirected graphs in this article (see Definition 1). Additionally, we consider graphs with only positive weights. This constraint comes from the fact that we aim here at recovering a real matrix $\widehat{\mathbf{T}}$ representing a diffusion process on a graph that explains the given signals.

Another important property of the normalized Laplacian, introduced by Chung [5], states that the eigenvalues of \mathbf{L} lie in the closed interval $[0, 2]$, with the multiplicity of eigenvalue 0 being equal to the number of connected components in the graph. From the definition of the diffusion matrix in Section II, we obtain that the eigenvalues of \mathbf{T} lie in the closed interval $[-1, 1]$, with at least one of them being equal to 1. If the graph

is connected then \mathbf{T} has a single eigenvalue equal to 1, being associated to a constant-sign eigenvector χ equal to:

$$\forall i \in \{1, \dots, N\} : \chi(i) = \sqrt{\frac{\mathbf{D}(i, i)}{\text{trace}(\mathbf{D})}}, \quad (5)$$

where \mathbf{D} is the matrix of degrees introduced in Section II, and all other eigenvalues of \mathbf{T} are strictly less than 1.

B. Characterization of the admissible diffusion matrices

Let us call $\mathcal{X}_{\mathbf{T}} = (\chi_1, \dots, \chi_N)$ the matrix of eigenvectors of \mathbf{T} . We have previously shown [17] that, in the limit case when M is infinite, the covariance matrix $\Sigma_{\mathbf{X}}$ of the given signals \mathbf{X} was equal to a particular (fixed) power K of the diffusion matrix. Thus, under this assumption, $\mathcal{X}_{\mathbf{T}}$ can be obtained at little cost using Principal Component Analysis on \mathbf{X} [21]. In the more global case when \mathbf{k} is a vector, the covariance matrix of the signals is a linear combination of multiple powers of \mathbf{T} , and has therefore the same set of eigenvectors, since all powers of a matrix share the same eigenvectors.

In more details, if we consider signals $\mathbf{x}_i = \mathbf{T}^{\mathbf{k}(i)} \mathbf{y}_i$, we have the following development. We note $\mathbf{X}(i)$ the signal at the i^{th} column of \mathbf{X} :

$$\begin{aligned} \widehat{\Sigma}_{\mathbf{X}} &= \sum_{i=1}^M \mathbf{X}(i) \mathbf{X}(i)^{\top} \\ &= \sum_{\mathbf{k} \in \mathbf{k}} \sum_{\substack{i \text{ s.t.} \\ \mathbf{k}(i) = \mathbf{k}}} \mathbf{X}(i) \mathbf{X}(i)^{\top} \\ &= \sum_{\mathbf{k} \in \mathbf{k}} \sum_{\substack{i \text{ s.t.} \\ \mathbf{k}(i) = \mathbf{k}}} \mathbf{T}^{\mathbf{k}} \mathbf{Y}(i) \mathbf{Y}(i)^{\top} \mathbf{T}^{\mathbf{k}\top} \\ &= \sum_{\mathbf{k} \in \mathbf{k}} \mathbf{T}^{\mathbf{k}} \left(\sum_{\substack{i \text{ s.t.} \\ \mathbf{k}(i) = \mathbf{k}}} \mathbf{Y}(i) \mathbf{Y}(i)^{\top} \right) \mathbf{T}^{\mathbf{k}\top} \\ \Sigma_{\mathbf{X}} &= \mathbb{E}_{\mathbf{Y}} \left[\sum_{i=1}^M \mathbf{X}(i) \mathbf{X}(i)^{\top} \right] \\ &= \sum_{\mathbf{k} \in \mathbf{k}} \mathbf{T}^{\mathbf{k}} \mathbb{E}_{\mathbf{Y}} \left[\sum_{\substack{i \text{ s.t.} \\ \mathbf{k}(i) = \mathbf{k}}} \mathbf{Y}(i) \mathbf{Y}(i)^{\top} \right] \mathbf{T}^{\mathbf{k}\top} \\ &= \sum_{\mathbf{k} \in \mathbf{k}} |\{i, \mathbf{k}(i) = \mathbf{k}\}| \mathbf{T}^{2\mathbf{k}}, \end{aligned} \quad (6)$$

which is a linear combination of various powers of \mathbf{T} , all having the same eigenvectors $\mathcal{X}_{\mathbf{T}}$.

Below we study the case when M is not high enough to allow for perfect retrieval of the eigenvectors of \mathbf{T} .

Given the remarks in Section IV-A, to recover an acceptable diffusion matrix $\widehat{\mathbf{T}}$, we must find a diagonal matrix $\widehat{\Lambda} = \text{diag}(\widehat{\lambda}_1, \dots, \widehat{\lambda}_N)$ of eigenvalues such that:

- $\widehat{\mathbf{T}} \triangleq \mathcal{X}_{\mathbf{T}} \widehat{\Lambda} \mathcal{X}_{\mathbf{T}}^{\top}$ is symmetric.
- $\forall i, j \in \{1, \dots, N\} : \widehat{\mathbf{T}}(i, j) \geq 0$.

Let us consider the randomly generated 3×3 symmetric adjacency matrix $\mathbf{W} = \begin{pmatrix} 0.417 & 0.302 & 0.186 \\ 0.302 & 0.147 & 0.346 \\ 0.186 & 0.346 & 0.397 \end{pmatrix}$. We compute its associated diffusion matrix \mathbf{T} , and its eigenvectors $\mathcal{X}_{\mathbf{T}}$. Let

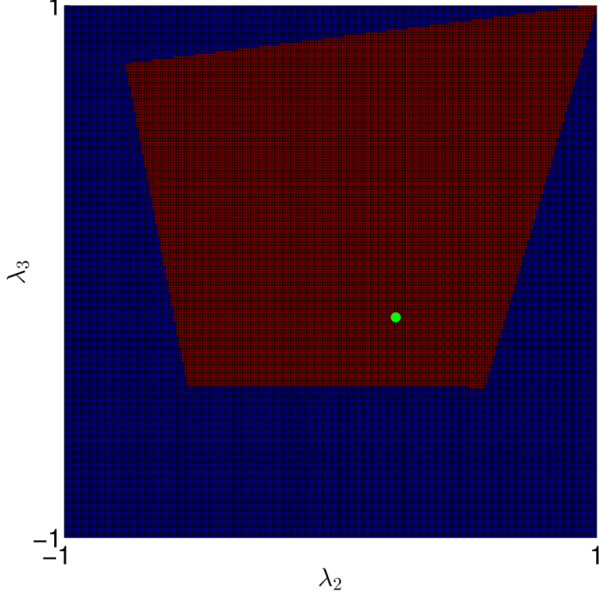


Figure 2. All pairs $(\lambda_2, \lambda_3) \in [-1, 1] \times [-1, 1]$ (using a step of 0.01) for which $\hat{\mathbf{T}} = \mathbf{X}_T \begin{pmatrix} 1 & 0 & 0 \\ 0 & \lambda_2 & 0 \\ 0 & 0 & \lambda_3 \end{pmatrix} \mathbf{X}_T^\top$ is a positive symmetric matrix (in red). Additionally, the exact eigenvalues of the diffusion matrix \mathbf{T} associated to \mathbf{W} are located using a green dot.

us set $\lambda_1 = 1$, with the associated χ_1 being the constant-sign eigenvector. For all pairs $(\lambda_2, \lambda_3) \in [-1, 1] \times [-1, 1]$ (using a step of 0.01), Fig. 2 depicts those that allow the reconstruction of a diffusion matrix verifying the two requirements above.

As we can see, the space of acceptable matrices is a convex structure, delimited by affine equations. To characterize these equations, let us consider any entry of index (i, j) in the matrix $\hat{\mathbf{T}}$ we want to recover. We can write this entry as a linear combination of variables $\lambda_1, \dots, \lambda_N$. Let $\alpha_{ij1}, \dots, \alpha_{ijN}$ be the factors associated to $\lambda_1, \dots, \lambda_N$ for $\hat{\mathbf{T}}(i, j)$. Enforcing the value of all entries of the matrix to be positive then defines the following set of inequalities:

$$\begin{aligned} \forall i, j \in \{1, \dots, N\}; j \geq i : \\ \alpha_{ij1}\lambda_1 + \alpha_{ij2}\lambda_2 + \dots + \alpha_{ijN}\lambda_N \geq 0, \end{aligned} \quad (7)$$

where $j \geq i$ comes from the symmetry property.

Our problem of recovering the correct set of eigenvalues to reconstruct the diffusion matrix thus becomes a problem of selecting a vector of dimension $N - 1$ (since one eigenvalue is equal to 1) in a convex polytope. Since the number of possible solutions is infinite; it is an ill-posed problem. To cope with this issue, in the next section we introduce some possible search strategies to find a set of eigenvalues enforcing potentially desirable properties on the reconstructed matrix.

V. STRATEGIES FOR RECOVERING A UNIQUE ADMISSIBLE DIFFUSION MATRIX

Now that we are able to characterize the space of acceptable eigenvalues for the diffusion matrix, we need to define some criteria to choose a particular solution of interest. An

appropriate criteria will generally depend on the application. In this section, we discuss two possibilities: recovering the diffusion matrix of a simple weighted graph, and recovering the diffusion matrix of a sparse graph. We give the details of each approach in the remainder of this section.

A. Recovering a simple graph

We have shown in (7) that the non-negativity of the entries in the reconstructed matrix can be enforced by a set of inequality constraints. A consequence is that if the reconstructed matrix contains any null entry, then the point we want to recover lies on an edge or a face of the polytope, since at least one inequality constraints holds with equality.

Suppose we want to recover a simple matrix, *i.e.*, a matrix having all elements on its diagonal being equal to 0. This property is useful in practical cases, because it enforces a diffusion process in which the vertices transmit all the signal energy to their neighbors, and do not retain part of it. Such a matrix has a trace equal to 0 and therefore, the sum of its eigenvalues is also 0.

To find a matrix verifying this property, a simple solution is to minimize the sum of the eigenvalues to recover. This can be done efficiently using the simplex algorithm [22]. A reason is that if the trace is null, then all values in the diagonal of the recovered matrix are equal to 0, due to the positivity constraints in (7). Therefore, the vector we want to recover is located at the intersection of multiple of these constraints. We state the linear programming problem as follows:

$$\begin{aligned} \hat{\lambda}_1, \dots, \hat{\lambda}_N = \arg \min_{\lambda_1, \dots, \lambda_N} \sum_{i=1}^N \lambda_i \\ \text{s. t. } \begin{cases} (7) \\ \forall i \in \{1, \dots, N\} : \lambda_i \in [-1, 1] \\ \lambda_1 = 1 \end{cases} \end{aligned} \quad (8)$$

with the two last constraints coming from the properties in Section IV-A. Enforcing $\lambda_1 = 1$ is not compulsory, but it imposes a scale factor, and reduces the problem dimension by one.

Let us consider the random 3×3 positive, symmetric and simple matrix $\mathbf{W} = \begin{pmatrix} 0 & 0.302 & 0.186 \\ 0.302 & 0 & 0.346 \\ 0.186 & 0.346 & 0 \end{pmatrix}$. Using the built-in MATLAB [23] function `linprog`, we solve the problem in (8) using the eigenvectors of the diffusion matrix \mathbf{T} associated to \mathbf{W} . Note that more elaborate commercial solvers such as Gurobi [24] or CPLEX [25] should perform much faster for larger instances of our problem.

Fig. 3 depicts the set of admissible pairs (λ_2, λ_3) as well as the exact eigenvalues and the recovered ones $(\hat{\lambda}_2, \hat{\lambda}_3)$ when solving (8) using the eigenvectors of \mathbf{T} . As we can see, the solution is a vector of the admissible space, and is located at the intersection of three constraints, since three entries of the initial matrix are null.

B. Recovering a sparse graph

In many applications one may believe the graph underlying the observations is sparse. Similar to the case when trying to recover a simple graph, finding a sparse admissible solution

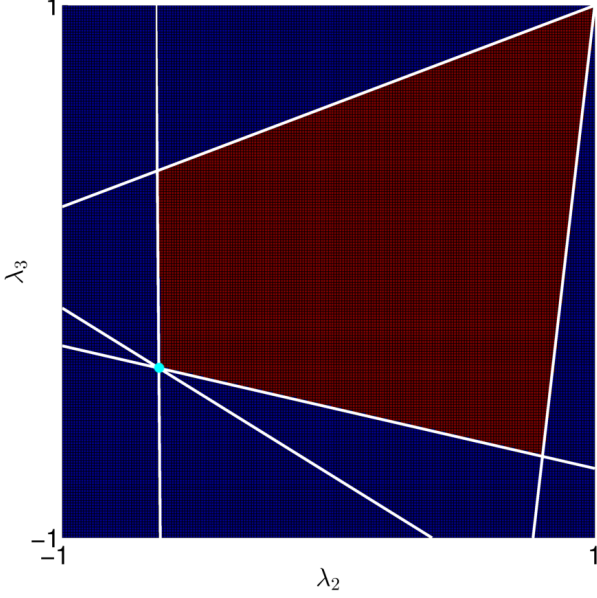


Figure 3. All pairs $(\lambda_2, \lambda_3) \in [-1, 1] \times [-1, 1]$ (using a step of 0.01) for which $\hat{\mathbf{T}} = \mathbf{X}_{\mathbf{T}} \begin{pmatrix} \lambda_1 & 0 & 0 \\ 0 & \lambda_2 & 0 \\ 0 & 0 & \lambda_3 \end{pmatrix} \mathbf{X}_{\mathbf{T}}^{\top}$ is a positive symmetric matrix (in red). The white lines represent the constraints defined in (7). The solution recovered by solving the linear program (8) coincide with the exact eigenvalues of the diffusion matrix \mathbf{T} associated with the matrix \mathbf{W} , and they are indicated by the green dot in the figure.

can be formulated as finding a point at the intersection of multiple linear constraints. To find a sparse solution, we seek the set of admissible eigenvalues for which the maximum number of constraints in (7) are null. This reduces to minimizing the ℓ_0 norm of the reconstructed matrix, which is known to be an NP-hard problem [26].

A common approach to circumvent this problem is to approximate the minimizer of the ℓ_0 norm by minimizing the ℓ_1 norm instead [27]–[29]. In this section, we adopt this approach and use again the simplex algorithm as follows:

$$\begin{aligned} & \hat{\lambda}_1, \dots, \hat{\lambda}_N = \\ & \arg \min_{\lambda_1, \dots, \lambda_N} \sum_{i=1}^N \sum_{j=1}^N \left(\mathbf{x}_{\mathbf{T}} \begin{pmatrix} \lambda_1 & 0 & 0 \\ 0 & \dots & 0 \\ 0 & 0 & \lambda_N \end{pmatrix} \mathbf{x}_{\mathbf{T}}^{\top} \right) (i, j) \\ & \text{s. t. } \begin{cases} (7) \\ \forall i \in \{1, \dots, N\} : \lambda_i \in [-1, 1] \\ \lambda_1 = 1 \end{cases} \end{aligned} \quad (9)$$

To solve this problem in our experiments, we use the CVX [30] package with solver SDPT3 [31] for MATLAB [23], with default parameters.

VI. EXPERIMENTAL RESULTS

In this section, we study the graph recovering strategies introduced in Section V. We first compare the results of our methods to other graph reconstruction algorithms on synthetic examples, and study the loss in precision for our methods when used with the empirical covariance matrix. Finally, we

apply our *Simple* technique on signals that are naturally one-dimensional, namely portions of a song, to assess its ability to recover a graph that we expect to be close to a path graph.

To assess our results, we compare the matrix reconstructed using our algorithms to a simple thresholded covariance matrix, and to the one recovered using the technique *GL-LogDet* proposed by Dong *et al.* [15]. We compare our method to theirs in two cases: when signals verifying the assumptions in [15] are observed, and when signals diffused on the graph are observed.

A. Performance metrics

To be able to evaluate the reconstruction error for all techniques, we use multiple metrics. Let \mathbf{T} be the ground truth diffusion matrix, with eigenvalues $\mathbf{\Lambda} = (\lambda_1, \dots, \lambda_N)$, and let $\hat{\mathbf{T}}$ be the one that is recovered using the assessed technique, with eigenvalues $\hat{\mathbf{\Lambda}} = (\hat{\lambda}_1, \dots, \hat{\lambda}_N)$.

The first metric we use is the mean error per reconstructed entry (MEPRE),

$$\text{MEPRE}(\mathbf{T}, \hat{\mathbf{T}}) \triangleq \frac{2}{N(N-1)} \sum_{i=1}^N \sum_{j=i}^N \left(\frac{\mathbf{T}(i, j)}{\|\mathbf{T}\|_F} - \frac{\hat{\mathbf{T}}(i, j)}{\|\hat{\mathbf{T}}\|_F} \right)^2. \quad (10)$$

This quantity represents the mean error for all entries in the triangular upper part of the reconstructed matrix, where we first normalize \mathbf{T} and $\hat{\mathbf{T}}$ using their Frobenius norm $\|\cdot\|_F$ to avoid biases related to a scale parameter.

To measure the reconstruction error of the retrieved eigenvalues (RERE), we compute the squared Euclidean distance between the ground truth eigenvalues and the recovered ones,

$$\text{RERE}(\mathbf{T}, \hat{\mathbf{T}}) \triangleq \frac{1}{N} \sum_{i=1}^N \left(\frac{\lambda_i}{\|\mathbf{\Lambda}\|_{\infty}} - \frac{\hat{\lambda}_i}{\|\hat{\mathbf{\Lambda}}\|_{\infty}} \right)^2. \quad (11)$$

Here, the normalization using $\|\cdot\|_{\infty}$ comes from the observation that the highest eigenvalue should be equal to 1. Therefore, it imposes a scale on the set of eigenvalues. Also, we divide the error by N to make it independent of the number of vertices.

Finally, we use a third metric representing the distance between the groundtruth eigenvalues and a power of the recovered ones. Since we assume that M is high enough to have $\Sigma_{\mathbf{x}} = \mathbf{T}^{2K}$ available, for an unknown $K \in \mathbb{R}$, then the algorithms should be able to recover at least a power of \mathbf{T} . Indeed, there is absolutely no way to distinguish for example one step of diffusion of a signal \mathbf{x} using \mathbf{T}^{2K} (i.e., $\mathbf{T}^{2K} \mathbf{x}$) and two diffusion steps of \mathbf{x} using \mathbf{T}^K (i.e., $(\mathbf{T}^K)^2 \mathbf{x}$). A consequence is that, if the algorithm cannot fully recover \mathbf{T} , it should at least recover a power of \mathbf{T} . Therefore, we define the reconstruction error of the powered retrieved eigenvalues (REPRE) as the Euclidean distance between the groundtruth vector of eigenvalues and the K -power of the recovered ones, for the best value of K possible,

$$\text{REPRE}(\mathbf{T}, \hat{\mathbf{T}}) \triangleq \min_{K \in \mathbb{R}} \frac{1}{N} \sum_{i=1}^N \left(\frac{\lambda_i^K}{\|\mathbf{\Lambda}^K\|_{\infty}} - \frac{\hat{\lambda}_i^K}{\|\hat{\mathbf{\Lambda}}\|_{\infty}} \right)^2. \quad (12)$$

B. Simulated networks

1) *Random graph models*: We first assess the two strategies we propose in Section V on well-controlled examples. We proceed in four steps:

- 1) We generate a random graph according to one of the models described below.
- 2) We compute its diffusion matrix \mathbf{T} .
- 3) For a random integer value of $K \in \{2, \dots, 5\}$, we compute \mathbf{T}^{2K} , and use it as the covariance matrix that would be obtained for an sufficiently high value of M .
- 4) Using only the knowledge of \mathbf{T}^{2K} (without knowing K), we apply the assessed method to recover $\hat{\mathbf{T}}$.

Then the recovered matrices are compared to the ground truth ones using the three metrics introduced in Section VI-A. All these steps are performed 100 times and we report the average performance.

We study the performances of the reconstruction techniques on two particular graph models to assess the impact of the graph structure on the results. The first model we consider is the Erdős-Rényi model [32], defined as follows:

Definition 4 (Erdős-Rényi graph): An Erdős-Rényi graph of parameter P is a random graph in which every edge has a probability P of existence. In the case of weighted graphs, we add a weight on the existing edges using an uniform distribution. The adjacency matrix of such a graph is defined by:

$$\mathbf{W}(u, v) = \mathbf{W}(v, u) \triangleq \begin{cases} \alpha_{uv} & \text{if } p_{uv} < P \text{ and } u \neq v \\ 0 & \text{otherwise} \end{cases};$$

$$\forall \{u, v\} \in \mathcal{V} \times \mathcal{V}; \quad \alpha_{uv} \sim \mathcal{U}(0, 1); \quad p_{uv} \sim \mathcal{U}(0, 1). \quad (13)$$

Another model we use to generate graphs is the random geometric model, defined as follows:

Definition 5 (Random geometric graph): A random geometric graph of parameter R is a graph built from a set of N uniformly distributed random points on the surface of a unitary torus, by adding an edge between those being closer than R according to the geodesic distance d on the torus. In the case of weighted graphs, we add a weight on the existing edges that is inversely proportional to the distance separating the points. Here, we choose to use the inverse of d . The adjacency matrix of such a graph is defined by:

$$\mathbf{W}(u, v) = \mathbf{W}(v, u) \triangleq \begin{cases} \frac{1}{d(u, v)} & \text{if } d(u, v) < R \text{ and } u \neq v \\ 0 & \text{otherwise} \end{cases};$$

$$\forall \{u, v\} \in \mathcal{V} \times \mathcal{V}. \quad (14)$$

Contrary to the Erdős-Rényi model, the random geometric graphs are by construction 2-dimensional. Also, they are frequently used to model connectivity in wireless networks [33].

Note that these two models describe sparse and simple graphs. Therefore, enforcing these two properties in our search strategies is sensible.

2) *Results using the exact eigenbasis*: Fig. 4 depicts the results obtained for 100 Erdős-Rényi graph of $N = 20$ vertices, with $P = 0.3$. All methods are assessed on the

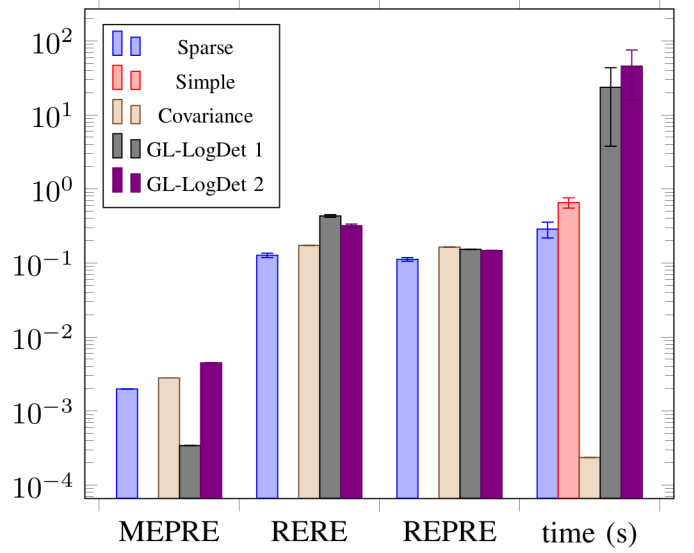


Figure 4. Mean results for 100 Erdős-Rényi graph of $N = 20$ vertices, with $P = 0.3$. Comparison of error measures, and median execution time per graph, for the five assessed algorithms. *Sparse* and *Simple* are the algorithms introduced in Section V. *Covariance* is a covariance matrix on which we apply a threshold equal to the maximum value such that every groundtruth edge appears in the recovered matrix. *GL-LogDet 1* and *GL-LogDet 2* are the application of the method of Dong et. al [15], respectively with signals according to their assumptions, and to ours.

same instances of graphs. In this figure, *Sparse* denotes the algorithm introduced in Section V-B, and *Simple* the one in Section V-A. The *Covariance* columns represent the errors obtained for a possible covariance matrix (i.e. \mathbf{T}^{2K} , for a random K) on which we apply the highest possible threshold such that every groundtruth edge appears in the thresholded matrix, regardless of the weights. Note that this method uses the knowledge of the groundtruth graph to find the best threshold, and is therefore not applicable *as is* in real cases. The two last columns of each group give the performance of the algorithm of Dong et. al [15]: *GL-LogDet 1* is the application of their method using their signals generating process, and *GL-LogDet 2* is the application of their algorithm using signals obtained after a few diffusions on the graph. For these two methods, the number of signals is chosen high enough for the method not to suffer from imprecisions, their generation is not included in the median execution time per graph, and the parameter α is set to 10.

Fig. 5 depicts the same results for 100 random geometric graphs of $N = 20$ vertices, with $R = 0.4$. The main difference with the results in Fig. 4 comes from the degree of sparsity $\frac{N^2 - \|\mathbf{W}\|_0}{N^2}$ of the considered graph, which is in general higher in the case of random geometric graphs with $R = 0.4$.

In both simulations, the *Simple* method perfectly recovered the diffusion matrices for the 100 test graphs, so the error measurements are not visible. From Fig. 4 and Fig. 5, it appears that the structure of the graph does not impact the relative performance of the various methods.

We also compare the median execution time per graph instance for the five methods, as a function of N . The results are given in Fig. 6, for random geometric graphs with $R = 0.4$.

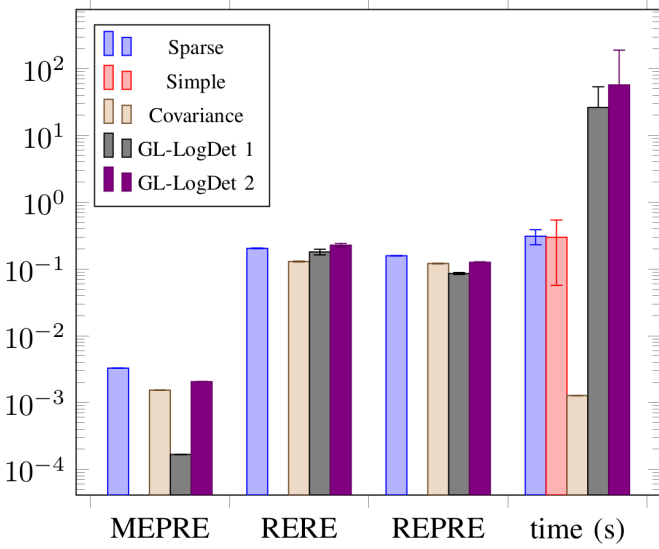


Figure 5. Mean results for 100 random geometric graph of $N = 20$ vertices, with $R = 0.4$. Comparison of error measures, and median execution time per graph, for the five assessed algorithms. *Sparse* and *Simple* are the algorithms introduced in Section V. *Covariance* is a covariance matrix on which we apply a threshold equal to the maximum value such that every groundtruth edge appears in the recovered matrix. *GL-LogDet 1* and *GL-LogDet 2* are the application of the method of Dong et. al [15], respectively with signals according to their assumptions, and to ours.

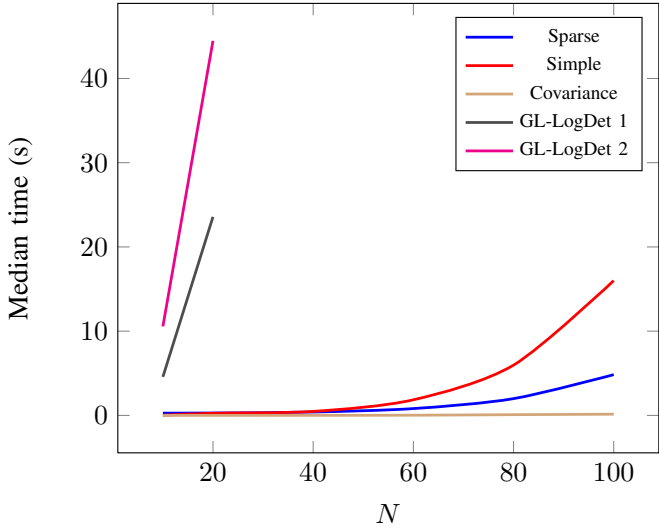


Figure 6. Median execution time per graph for the five compared methods, on random geometric graph with $R = 0.4$. For each value of N , the time given is a mean for 100 random graphs. Due to their complexity, *GL-LogDet 1* and *GL-LogDet 2* are plotted for graphs of up to $N = 20$ vertices.

We have chosen this graph model with a fixed radius to keep a constant sparsity degree across all graphs. Also, we represent the median time per graph and not the mean time because there happens to be a few outlier graphs for which the execution time increases a lot, as it can be seen from the time variance in Fig. 4 and Fig. 5. However, such cases are really marginal, and would cause less representative results if plotting the mean times.

Numerous interesting observations can be made from these simulations. First, as expected, a simple thresholding process

of the covariance matrix is not sufficient to recover the original diffusion matrix. This can be seen from the error measurements in both Fig. 4 and Fig. 5. Although the method is fast, this justifies the need for more elaborate techniques.

The results of the *Simple* method are very good, as the method succeeds at recovering the initial matrix in almost all cases (we observed a small error $\text{RERE} = 10^{-6}$ in very few simulations when measuring the execution time for $N = 100$, probably caused by machine precision issues). Also, its median execution time per graph is quite low, due to the efficiency of solving a linear programming problem. Additionally, while being slightly slower than the *Sparse* method, *Simple* scales quite well, and can be applied to graphs with a decent number of vertices, as can be seen in Fig. 6.

When considering the reference methods, the *GL-LogDet 1* technique efficiently manages to recover a matrix that is similar to the diffusion matrix, but that has a very different spectral decomposition. The difference between *GL-LogDet 1* and *GL-LogDet 2* comes from the input signals. The first method uses signals satisfying the assumptions in [15], while the second one takes signals diffused on the graph as an input. As we can see in both Fig. 4 and Fig. 5, the method *GL-LogDet 2* does not apply under our assumptions, and provides results that are comparable to a simple covariance matrix thresholding. Therefore, the application of *Simple* or *GL-LogDet 1* is dependent on the assumptions on the input signals.

Finally, let us discuss results for the *Sparse* method. When looking at the results in Fig. 4 and Fig. 5, the method seems to provide low-quality results. As a matter of fact, there are numerous sets of eigenvalues that lead to admissible sparse matrices. Every vertex of the polytope is therefore a possible solution, and none of them is better than another one, unless some polytope vertices are at the intersection of more inequalities than the others.

To illustrate this, let us consider an example 3×3 sparse matrix. The polytope in Fig. 7 depicts the admissible pairs (λ_2, λ_3) for this matrix, as we did in Fig. 3.

As we can see, the *Sparse* method recovers a matrix with two null entries in the triangular upper part, which matches the structure of the ground truth matrix. This suggests that if the *Sparse* method fails to recover the correct solution, then it will also be far, in most cases, from any power of the ground truth diffusion matrix. In conclusion, the *Sparse* method is not sufficient to properly select a matrix, and should be used with additional priors to distinguish between all possible solutions.

3) *Results when estimating the eigenbasis:* The results discussed above use the exact covariance matrix Σ_X , directly obtained by elevating the diffusion matrix of the graph under study to a certain even power. Next, we study the impact of the use of the empirical covariance matrix $\hat{\Sigma}_X$ of controlled signals respecting our assumptions. In practice, we only need the eigenvectors $\mathcal{X}_{\hat{\Sigma}_X} = (\hat{x}_1, \dots, \hat{x}_N)$ of this matrix, which we can obtain using PCA on the signals.

To understand the impact of using by $\hat{\Sigma}_X$ instead of Σ_X , let us again consider an example 3×3 matrix and the associated polytope. We generate a random graph with $N = 3$ vertices and compute its diffusion matrix T . Using T , we

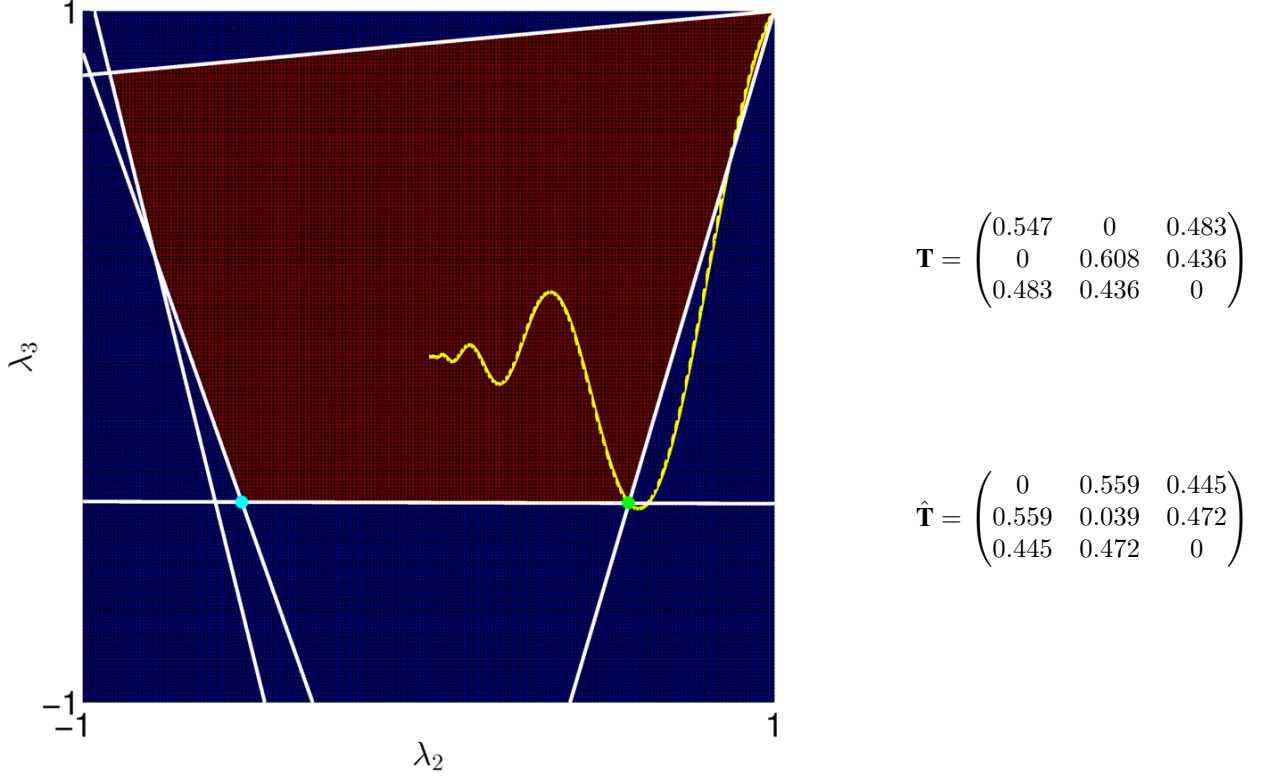


Figure 7. Polytope associated with the 3×3 matrix to the right (top). The ground truth eigenvalues are located at the bottom-right corner, while the recovered ones are at the bottom-left one. The yellow trace represents the various powers of the ground truth eigenvalues; *i.e.*, λ_i^K for numerous values of K . To the right of the figure, the top matrix is the ground truth diffusion matrix, and the bottom one the recovered one.

diffuse M mutually independent signals with independent entries a variable number of times to obtain \mathbf{X} . Then, we compute the empirical covariance matrix of \mathbf{X} , and determine its eigenvector $\mathcal{X}_{\hat{\Sigma}_{\mathbf{X}}}$.

Fig. 8 depicts the ground truth polytope (*i.e.*, the one associated to the eigenvectors of $\Sigma_{\mathbf{X}}$) and the polytopes associated to 10 different $\hat{\Sigma}_{\mathbf{X}}$, obtained from multiple realizations of \mathbf{X} . From each of the eigenvector sets of these empirical covariance matrices, we determine the pairs (λ_2, λ_3) that satisfy the criteria in Section IV-B. Then, we plot a histogram of the number of occurrences of these valid pairs.

As we can see, visually the recovered polytope more accurately reflects the true one as M increases. This coincides with the fact that the empirical covariance matrix converges to the real one as M tends to infinity.

Now, let us study the error when compared to the ground truth matrix. We have seen in Section VI-B2 that the *Simple* method could efficiently recover the angle in the polytope that minimizes the trace. Therefore, we can use this method to find this particular point in the empirical polytopes, and evaluate the MEPRE. Contrary to the previous simulations, studying RERE and REPRES is not really relevant, since the eigenvalues are not defined in the exact same eigenspace. In Fig. 9, we study the MEPRE of the recovered graphs using $\hat{\Sigma}_{\mathbf{X}}$, for multiple values of M . We consider mean results on 100 random geometric graphs of $N = 10$ vertices. The

studied signals are obtained for a random number of diffusions (from 2 to 5) of initially mutually independent signals with independent entries. Although the results apply for any vector \mathbf{k} , we may face a problem in the case when the signals are diffused too many times. In this case, since the eigenvalues of \mathbf{T} are in the interval $[-1, 1]$, then their contributions in the signals spectrum are removed due to limited machine precision.

Sometimes, the polytope appears to be empty due to the imprecision of the eigenvectors obtained by PCA. In such cases, we perform the experiment again by relaxing the inequality constraints in (7) a bit, *i.e.*, by allowing the entries of the recovered matrix to be higher than $-\varepsilon$ instead of 0, for increasing values of ε , until the polytope becomes non-empty. Also, for the *GL-LogDet* method, we test multiple values of α and keep the best one.

The results show that the *Simple* method succeeds quite well in recovering a graph that is close to the initial one. As expected, the quality of the recovery is a function of the number of signals, and a high value of M leads to a better recovery. In most cases, the correct angle of the polytope is chosen by the method, and the retrieved solution differs from the groundtruth one mainly due to the imprecisions in the eigenvectors retrieval.

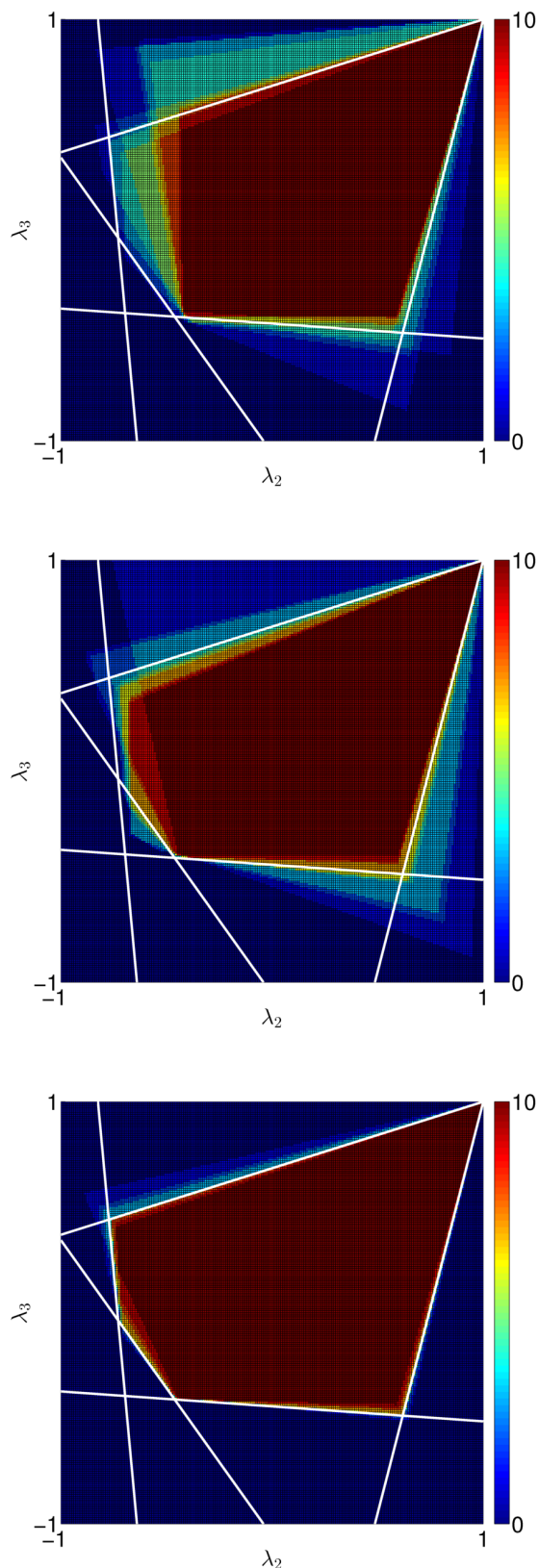


Figure 8. The groundtruth polytope is represented by the inequality constraints in white. The z axis (represented with colors) represents the number of times a pair (λ_2, λ_3) is valid, in the sense of the criteria in Section IV-B, when used jointly with \mathcal{X}_{Σ_X} to recover a diffusion matrix. Results obtained for 10 instances of \mathbf{X} on the same graph, for $M = 10$ (top), $M = 100$ (middle) and $M = 1000$ (bottom).

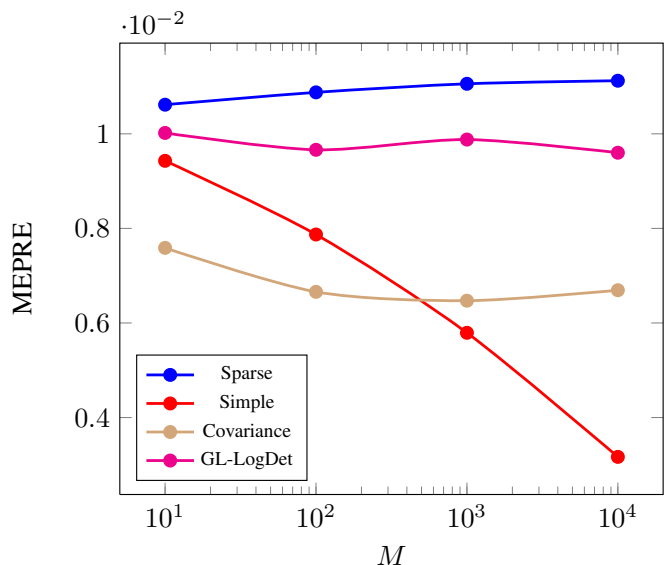


Figure 9. MEPRE obtained for the assessed techniques on random geometric graphs with $N = 10$ vertices, for multiple values of M . Mean for 100 graphs per value of M .

C. Real data: Audio signals

The hypothesis of the proposed method is that observed signals are obtained through diffusion of mutually independent signals with independent entries over a graph. A direct consequence is that structure of the signals can only be explained thanks to the graph. We perform a simple validation test to stress this property. We take as input audio signals obtained by sampling a song at a frequency of 44,100 Hz and partitioning the result into groups of consecutive samples. Since the signals are assumed to be initially independent, the recovered structure should be one-dimensional and resemble a line graph.

Fig. 10 illustrates the result of our method, *Simple* applied on signals obtained by cutting the song *Around the World* by the band Daft Punk into portions of $N = 50$ consecutive frames (*i.e.*, each lasting roughly 1 ms). This gives us a set of 378,593 signals. We then compute the covariance matrix of these signals and diagonalize it to obtain its eigenvectors.

As we can see, our method succeeds at recovering a matrix that is one-dimensional. Also, from Fig. 10 (c) and (d), we observe that the recovered matrix gives less importance to the edges that link vertices corresponding to non-adjacent times than the covariance matrix does.

VII. CONCLUSIONS

In this article we have demonstrated that, given a set of signals that we assume to be produced from a few steps of diffusion of mutually independent signals with independent entries on a graph, we can retrieve the graph used for the diffusion. We use the fact that the eigenvectors of the covariance matrix of the signals are the same as those of the matrix used for the diffusion. We have shown that the set of eigenvalues to associate to these eigenvectors that lead to admissible matrices forms a convex polytope. Finding a graph then reduces to selecting a point in this convex structure. We have proposed two methods for doing so, respectively emphasizing

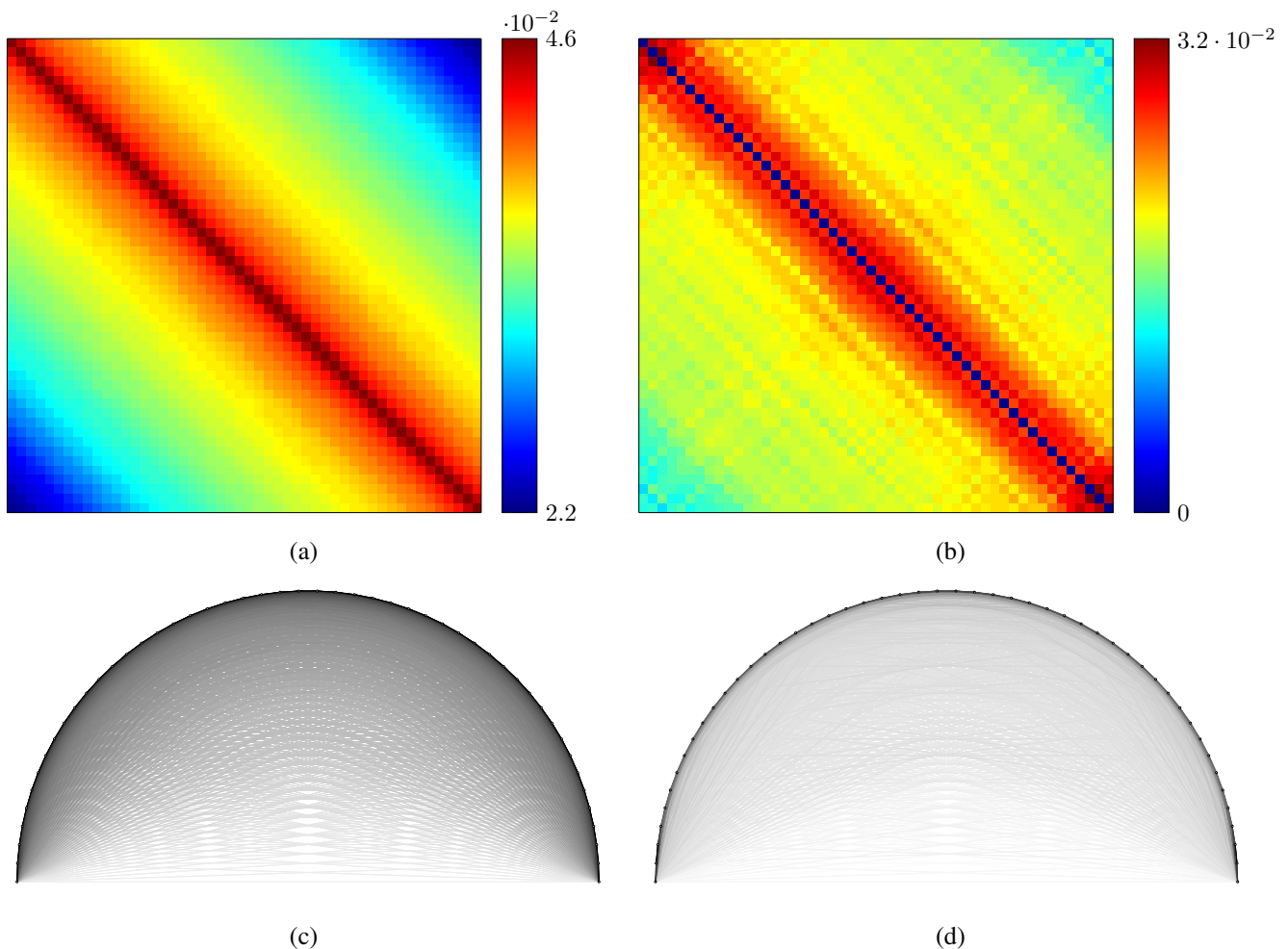


Figure 10. (a) Covariance matrix of the signals obtained by partitioning the song. The colors in the cells represent the values of the associated matrix entries, with the highest ones being red and the smallest ones blue. (b) Result diffusion matrix obtained with the *Simple* algorithm. (c) Representation of the covariance matrix as a graph. Vertices are placed regularly on the top half of a circle, and edges are added with a color intensity that is function of the intensity of the connection in the matrix. (d) Representation of the result of the *Simple* method as a graph.

the recovery of either a simple or a sparse graph. Both methods admit computationally efficient implementation, since they are respectively based on solving a linear programming problem and on solving a linear optimization problem.

In the limit case, when we have the exact covariance matrix, we are able to recover the graph with no error. In more realistic cases, we have shown in synthetical examples that our method is able to find a graph that is very close to the ground truth one. To illustrate the applicability of our method, we have used it on audio signals, and have shown that we were able to recover a graph that is globally one-dimensional.

Future directions based on this work are numerous. First of all, we could explore new strategies to select a set of admissible eigenvalues, for example by enforcing the reconstruction of a binary matrix. Also, while the proposed selection methods *Sparse* and *Simple* perform quite fast, defining the $\frac{N(N-1)}{2}$ constraints enforcing the positivity of the reconstructed matrix takes some time. An interesting direction would then be to propose selection strategies that do not imply the full definition of these constraints. Finally, our direct next work will be to investigate how the graphs obtained with our methods can help

in problems such as classification, by using the graph structure to improve the performance of classical methods.

ACKNOWLEDGEMENTS

The authors would like to particularly thank Xiaowen Dong for providing code to implement the methods from [15]. Additionally, we would like to thank Pierre Vanderghenst and his group at EPFL for the inspiring discussions.

REFERENCES

- [1] F. D. V. Fallani, J. Richiardi, M. Chavez, and S. Achard, "Graph analysis of functional brain networks: Practical issues in translational neuroscience," *Phil. Trans. R. Soc. B*, vol. 369, no. 1653, p. 20130521, 2014.
- [2] G. Camps-Valls, T. V. B. Marsheva, and D. Zhou, "Semi-supervised graph-based hyperspectral image classification," *Geoscience and Remote Sensing, IEEE Transactions on*, vol. 45, no. 10, pp. 3044–3054, 2007.
- [3] R. Mazumder and T. Hastie, "Exact covariance thresholding into connected components for large-scale graphical lasso," *The Journal of Machine Learning Research*, vol. 13, no. 1, pp. 781–794, 2012.
- [4] J. Friedman, T. Hastie, and R. Tibshirani, "Sparse inverse covariance estimation with the graphical lasso," *Biostatistics*, vol. 9, no. 3, pp. 432–441, 2008.
- [5] F. R. Chung, *Spectral Graph Theory*. American Mathematical Soc., 1997, vol. 92.

- [6] D. I. Shuman, S. K. Narang, P. Frossard, A. Ortega, and P. Vandergheynst, "The emerging field of signal processing on graphs: Extending high-dimensional data analysis to networks and other irregular domains," *Signal Processing Magazine, IEEE*, vol. 30, no. 3, pp. 83–98, 2013.
- [7] A. P. Dempster, "Covariance selection," *Biometrics*, pp. 157–175, 1972.
- [8] A. J. Rothman, P. J. Bickel, E. Levina, J. Zhu *et al.*, "Sparse permutation invariant covariance estimation," *Electronic Journal of Statistics*, vol. 2, pp. 494–515, 2008.
- [9] D. M. Witten, J. H. Friedman, and N. Simon, "New insights and faster computations for the graphical lasso," *Journal of Computational and Graphical Statistics*, vol. 20, no. 4, pp. 892–900, 2011.
- [10] R. Mazumder and T. Hastie, "The graphical lasso: New insights and alternatives," *Electronic Journal of Statistics*, vol. 6, p. 2125, 2012.
- [11] K. M. Tan, D. Witten, and A. Shojaie, "The cluster graphical lasso for improved estimation of gaussian graphical models," *Computational Statistics & Data Analysis*, vol. 85, pp. 23–36, 2015.
- [12] S. Huang, J. Li, L. Sun, J. Liu, T. Wu, K. Chen, A. Fleisher, E. Reiman, and J. Ye, "Learning brain connectivity of alzheimer's disease from neuroimaging data," in *Advances in Neural Information Processing Systems*, 2009, pp. 808–816.
- [13] S. Yang, Q. Sun, S. Ji, P. Wonka, I. Davidson, and J. Ye, "Structural graphical lasso for learning mouse brain connectivity," in *Proceedings of the 21th ACM SIGKDD International Conference on Knowledge Discovery and Data Mining*, 2015, pp. 1385–1394.
- [14] S. Sun, R. Huang, and Y. Gao, "Network-scale traffic modeling and forecasting with graphical lasso and neural networks," *Journal of Transportation Engineering*, vol. 138, no. 11, pp. 1358–1367, 2012.
- [15] X. Dong, D. Thanou, P. Frossard, and P. Vandergheynst, "Learning laplacian matrix in smooth graph signal representations," *arXiv preprint arXiv:1406.7842*, 2014.
- [16] P. K. Shivaswamy and T. Jebara, "Laplacian spectrum learning," in *Machine Learning and Knowledge Discovery in Databases*. Springer, 2010, pp. 261–276.
- [17] B. Pasdeloup, M. Rabbat, V. Gripon, D. Pastor, and G. Mercier, "Graph reconstruction from the observation of diffused signals," in *Proceedings of the 53rd Annual Allerton Conference on Communication, Control, and Computing*, 2015.
- [18] M. Ipsen and A. S. Mikhailov, "Evolutionary reconstruction of networks," *Physical Review E*, vol. 66, no. 4, p. 046109, 2002.
- [19] A. Agaskar and Y. M. Lu, "A spectral graph uncertainty principle," *Information Theory, IEEE Transactions on*, vol. 59, no. 7, pp. 4338–4356, 2013.
- [20] N. Tremblay, "Réseaux et signal: des outils de traitement du signal pour l'analyse des réseaux," Ph.D. dissertation, Ecole Normale Supérieure de Lyon, 2014.
- [21] K. Pearson, "On lines and planes of closest fit to system of points in space," *Philosophical Magazine*, vol. 2, pp. 559–572, 1901.
- [22] G. B. Dantzig, in *A History of Scientific Computing*, S. G. Nash, Ed. New York, NY, USA: ACM, 1990, ch. Origins of the Simplex Method, pp. 141–151.
- [23] MATLAB, version 7.14.0 (R2012a). Natick, Massachusetts: The MathWorks Inc., 2012.
- [24] I. Gurobi Optimization, "Gurobi optimizer reference manual," 2015. [Online]. Available: <http://www.gurobi.com>
- [25] I. C. 1987, "IBM ILOG CPLEX optimization studio CPLEX user's manual," <http://www-03.ibm.com/software/products/en/ibmilogcplexoptstud>, 2014.
- [26] E. Amaldi and V. Kann, "On the approximability of minimizing nonzero variables or unsatisfied relations in linear systems," *Theoretical Computer Science*, vol. 209, no. 1, pp. 237–260, 1998.
- [27] S. S. Chen, D. L. Donoho, and M. A. Saunders, "Atomic decomposition by basis pursuit," *SIAM Review*, vol. 43, no. 1, pp. 129–159, 2001.
- [28] R. Gribonval and M. Nielsen, "Sparse representations in unions of bases," *Information Theory, IEEE Transactions on*, vol. 49, no. 12, pp. 3320–3325, 2003.
- [29] F. Rinaldi, "Mathematical programming methods for minimizing the zero-norm over polyhedral sets," Ph.D. dissertation, Sapienza, University of Rome, 2009.
- [30] M. Grant and S. Boyd, "CVX: MATLAB software for disciplined convex programming, version 2.1," <http://cvxr.com/cvx>, Mar. 2014.
- [31] K. C. Toh, M. Todd, and R. H. Tütüncü, "SDPT3 – a MATLAB software package for semidefinite programming," *Optimization Methods and Software*, vol. 11, pp. 545–581, 1999.
- [32] P. Erdős and A. Rényi, "On random graphs I," *Publ. Math. Debrecen*, vol. 6, pp. 290–297, 1959.
- [33] M. Nekovee, "Worm epidemics in wireless ad hoc networks," *New Journal of Physics*, vol. 9, no. 6, p. 189, 2007.